# Integrated design and allocation of optimal aircraft departure routes

Ho-Huu, V.; Hartjes, S.; Visser, H. G.; Curran, R.

**DOI**
10.1016/j.trd.2018.07.006

**Publication date**
2018

**Document Version**
Accepted author manuscript

**Published in**
Transportation Research Part D: Transport and Environment

# Integrated design and allocation of optimal aircraft departure routes

V. Ho-Huu*, S. Hartjes, H. G. Visser, R. Curran

*Faculty of Aerospace Engineering, Delft University of Technology, Delft, The Netherlands*
E-mails: v.hohuu@tudelft.nl; vinh.ho.h@gmail.com (V. Ho-Huu), s.hartjes@tudelft.nl (S. Hartjes), h.g.visser@tudelft.nl (H. G. Visser), r.curran@tudelft.nl (R. Curran)

## Abstract

This paper presents a new multi-objective optimization formulation for the design and allocation of optimal aircraft departure routes. In the considered problem – besides two conventional objectives based on cumulative noise criteria and fuel burn – a new objective considering the flight frequency is introduced. Moreover, to take advantage of the combination of designing new routes and allocating flights to these routes, two different routes are considered simultaneously, and the distribution of flights over these two routes is addressed in parallel. Then, a new version of the so-called MOEA/D optimization algorithm is developed to solve the formulated optimization problem. Two different case studies, one at Rotterdam The Hague Airport and one at Amsterdam Airport Schiphol in The Netherlands, are carried out to evaluate the reliability and applicability of the proposed approach. The obtained results reveal that the proposed approach can provide solutions which can balance more effectively the concerned metrics such as the number of annoyed people, fuel burn, number of people exposed to certain noise levels, and number of aircraft movements which people are subjected to.

**Keywords**: departure routes; trajectory optimization; allocation optimization; noise abatement; noise events, fuel consumption.

* Corresponding author: V. Ho-Huu, e-mails: v.hohuu@tudelft.nl; vinh.ho.h@gmail.com

## 1. Introduction

With a significant impact on economic development, communication, tourism and job creation, aviation is predicted to grow quickly in the coming years (Boeing, 2016). In response to this trend, airports are forced to increase their operations, and hence a significantly increasing amount of aircraft movements needs to be handled every day. Nevertheless, the expansion of these activities often causes harmful effects on local communities such as noise and pollutant emissions (Hartjes et al., 2014). This leads to an adverse community reaction to authorities and policymakers, resulting in opposition to the extension of airport and aircraft operations. Thus, it is crucial to identify solutions to aid the sustainable development of the aviation industry, while minimizing its adverse impact as much as possible.

In an effort to overcome the above issues, a series of research initiatives has been launched in recent years, e.g. Clean Sky[†], AIRE[‡], and ASPIRE[§]. Apart from these research initiatives, a number of different approaches have also been proposed – and are currently being implemented – such as creating new criteria and regulations, advancing new engine/aircraft models and replaceable fuels, and varying operational procedures of aircraft and airports (Marais et al., 2013). From a practical implementation point of view, it can be observed that the variation of aircraft/airport operational procedures emerges as a suitable option that can result in short term improvements and could be less costly in comparison with the other options. For this approach, the optimal design of routes for departures and arrivals, and the allocation of aircraft to these routes are considered as the most promising options (Green, 2005).

The literature shows that efforts to design optimal departure and arrival routes with less noise and fuel burn have been well studied over the past decades, and various strategies have been proposed. For example, the optimization tool NOISHHH, a combination of a dynamic trajectory optimization method, a noise model, an inventory model of emissions and a Geographic Information System (GIS), was developed by Visser and Wijnen (2003, 2001) to create environmentally optimal departure and arrival trajectories. This tool was extended over the years for amongst others the design of optimal terminal routes based on area navigation (Braakenburg et al., 2011; Hartjes et al., 2010; Hogenhuis et al., 2011). A lexicographic optimization approach was utilized by Prats et al. (2011, 2010a, 2010b) to optimize aircraft departure trajectories with noise annoyance criteria. In an effort to reduce noise impact, Khardi and Abdallah (2012) carried out a comparison study of direct and indirect approaches for solving the system of ordinary differential equations (ODEs) to generate optimal aircraft flight paths. Torres et al. (2011) applied a gradient-free optimization method called multi-objective mesh adaptive direct search (multi-MADS) to create optimal departure trajectories with less noise and $NO_x$-emissions at a single measurement point. Hartjes and Visser (2016) proposed a novel trajectory parameterization technique, and then applied the elitist non-dominated sorting genetic algorithm (NSGA-II) to design environmentally friendly departure trajectories. Later, this technique was also utilized to design departure routes at Manchester Airport by Zhang et al. (2016). Recently, a multi-

[†] Clean Sky. http://www.cleansky.eu/#no-back. (accessed 23 October 2017).

[‡] Atlantic Interoperability Initiative to Reduce Emissions (AIRE). https://ec.europa.eu/- transport/modes/air/environment/aire_en, (accessed 23 October 2017).

[§] Asia and South Pacific Initiative to Reduce Emissions (ASPIRE). http://www.aspire-green.com/, (accessed 23 October 2017).

objective evolutionary algorithm based on decomposition (MOEA/D) was developed by Ho-Huu et al. (2017, 2018a) to design optimal departure routes with less noise and fuel burn.

Besides the attempts to design environmentally friendly departure/arrival routes, the allocation of aircraft and operational procedures to specific routes could also help to considerably diminish the environmental impacts. For instance, Frair (1984) proposed a nonlinear integer programming model to minimize community annoyance at an airport by allocating aircraft to the existing arrival and departure trajectories. Zachary et al. (2010) investigated the optimization problem which aims at finding an optimal combination of approach and departure routes, operational procedures and fleet composition to optimize noise and pollutant emissions. Kuiper et al. (2012) developed an optimization tool for allocating and distributing the annual aircraft movements over available runways and routes to maximize the allowable number of flight operations into and out of an airport within a given annual noise budget. Kim et al. (2014) built an optimization model to minimize the total emissions on the airport surface and in the terminal area by allotting aircraft to runways and scheduling the arrival and departure operations on these runways concurrently.

Looking at the above literature review on the design of arrival and departure routes, the studies can be generally categorized into two different groups: those using single-event noise criteria (Hartjes et al., 2010; Ho-Huu et al., 2017; Hogenhuis et al., 2011; Prats et al., 2010a, 2010b; Torres et al., 2011; Visser & Wijnen, 2001, 2003) and those using multi-event or cumulative noise criteria (Braakenburg et al., 2011; Hartjes et al., 2014). For the first group, the most widely used criterion is to minimize the number of people awakened, which is derived from either the Federal Interagency Committee on Aviation Noise (FICAN, 1997) or later the American National Standards Institute (ANSI, 2008). Although results can be obtained for different types of aircraft, the resulting optimal routes are most likely only suitable for that specific aircraft. This is because the noise criteria are evaluated based on a specific aircraft model. From an airport operations or Air Traffic Control point of view, however, it is not feasible to manage individual routes for individual aircraft types. For the second group, the most broadly used criterion is to minimize the number of people annoyed, where dose-response relationships based on the day-evening-night noise level ($L_{\mathrm{den}}$) or night noise level ($L_{\mathrm{night}}$) are often employed (Braakenburg et al., 2011; Hartjes et al., 2014). Unlike the first approach, these noise criteria are determined based on the aggregation of noise caused by different aircraft types, where the number of aircraft movements is also taken into account. Therefore, the optimal routes obtained can be applied for different aircraft types and depend on an assumed fleet mix. Though the optimal solutions do not fully exploit the potential noise reduction for each individual aircraft type because of the requirements to follow a common path, from an operational perspective this approach is easier to implement.

From the studies using the second approach, it is also identified that all studies design only one optimal route at a time, and all aircraft movements have to follow the same common path. Although the multi-event noise metrics have already included the influence of the number of aircraft movements, they do not explicitly take into account the frequency of those events. Though noise levels will increase with increasing aircraft movements, and consequently the number of people highly annoyed will increase as well, it is conceivable that an increase in the number of movements above a certain level may lead to more resistance in local communities than the common dose-response relationships would predict. This issue has recently been recognized as one of the emerging concerns that should be investigated and taken into account in noise regulations and policies (Brown, 2014; Fields, 1984; Janssen et al., 2014). In addition, recent studies have also pointed out that despite playing an important role in noise assessment, the above metrics contain certain limitations (Porter et al., 2014; Southgate, 2011). Most importantly, these metrics do not represent the actual experience of communities who are not noise experts, and hence it is difficult for authorities and decision makers to communicate related policies to the local communities (Porter et al., 2014; Southgate, 2011). As a consequence, they have been regularly considered as unhelpful and lacking transparency (Porter et al., 2014; Southgate, 2011). In order to address this issue, the Australian Government developed supplementary noise descriptor concepts that can help the general public to understand and communicate with the authorities (DOTARS, 2000). They include the numbers of events above certain noise levels (N70s, N65s), Person Event Index (PEI) and Average Individual Exposure (AIE), which are helpful to provide simple information on the location of flight paths, the number of aircraft movements and the time of day of the movements. Nowadays, these metrics have been recognized and widely used in many countries in the world such as Austria, Sweden and the United Kingdom (Porter et al., 2014). So far, these metrics are, however, rarely considered for designing new aircraft routes.

In an attempt to generate optimal departure routes which can balance the above concerns more effectively, in this paper we have developed a new approach for the optimum design and allocation of departure routes. In the formulation of optimization problems, besides a conventional noise objective derived from cumulative noise criteria (i.e., the number of people annoyed) and fuel burn, a new objective considering the frequency of noise events is developed. While the first and second objectives can be obtained by designing only one route as in traditional approaches (Braakenburg et al., 2011; Hartjes et al., 2014), to minimize the third objective and essentially to distribute the noise impact, evidently at least two alternative routes are needed. For this reason, in the proposed optimization problem two alternative routes will be considered at the same time, and the allocation of flights to these two routes will be optimized concurrently. Furthermore, to make the approach more generic, two different departure procedures currently in use, namely, Noise Abatement Departure Procedure 1 and 2 (NADP1, NADP2) (ICAO, 2006) are utilized and considered as design variables as well.

With the above considerations, a multi-objective optimization problem with three objectives is formulated. It can be recognized that this is a nonlinear multi-objective optimization problem with mixed discrete-continuous design variables, where the continuous variables relate to the coordinates of the two routes, based on the regulations of the International Civil Aviation Organization (ICAO, 2006), while the discrete variables are the number of flights on each route and the selection of one of the two noise abatement departure procedures, i.e. NADP1 or NADP2. In addition, the optimization problem has both equality and inequality constraints, which are the restrictions on the total number of flights and on aircraft performance, such as bank angle constraints. Generally, this is a complicated optimization problem that needs a specific algorithm for resolution. In this study, a new version of the algorithm called multi-objective optimization based on decomposition (MOEA/D), which has been developed recently by the authors in Ho-Huu et al. (2017, 2018a) is extended to address this problem. Nevertheless, compared with the problems in Ho-Huu et al. (2017), besides the inequality constraints the problem in this study contains both equality constraints and mixed discrete-continuous design variables. Therefore, to increase the performance of the algorithm, techniques for handling the equality constraints and the mixed discrete-continuous variables are also proposed.

The reliability, effectiveness and applicability of the proposed approach are demonstrated through two different case studies in The Netherlands. The first one is a scenario at a regional airport, *viz.* Rotterdam The Hague Airport (RTM), and the second example is a case study at one of the busiest airports in the world, *viz.* Amsterdam Airport Schiphol (AAS). The obtained simulation results indicate that the proposed approach can provide optimal solutions which offer a good trade-off between the concerned metrics.

The rest of the paper is structured as follows. Section 2 presents the formulation of the multi-objective optimization problem. Section 3 gives a brief overview of the trajectory parameterization technique and aircraft performance modeling. Section 4 describes the optimization algorithm and two techniques for handling the equality constraints and mixed discrete-continuous design variables. The numerical examples are presented in Section 5, and finally some conclusions and are stated in Section 6.

## 2. Multi-objective optimization problem formulation

As discussed above, to generate optimal departure routes which can effectively handle the concerns of policymakers, airlines and communities, besides the traditional objectives like the number of people annoyed and fuel burn, it is relevant to include objectives which can take into account the frequency of aircraft noise events. Therefore, a new optimization objective which considers this concern is developed in this study. In general, the mathematical model of an optimization problem with three objectives is stated as follows:

$$\begin{aligned} \min_{\mathbf{d}} \quad & \left(f_1(\mathbf{d}), f_2(\mathbf{d}), f_3(\mathbf{d})\right) \\ \text{s.t.} \quad & \sum_{j=1}^{2} a_{ij} = \mathrm{T}_{\mathrm{at},i}, \ i = 1,..,N_{\mathrm{at}} \\ & \mu_i(t) \le \mu_{\max}(h) \end{aligned} \tag{1}$$

where $\mathbf{d} = \{\mathbf{g}, \mathbf{a}, \mathbf{p}\}$ is the design variable vector of the optimization problem, in which $\mathbf{g}$ is the vector of variables defining the geometric parameters of two departure routes, $\mathbf{a}$ is the vector of aircraft allocation to each route (in which $a_{ij}$ is the number of aircraft type $i$ on route $j$) and $\mathbf{p}$ is the vector of noise abatement departure procedures of aircraft type $i$ on route $j$. The parameters $N_{\mathrm{at}}$ and $T_{\mathrm{at},i}$ are, respectively, the number of aircraft types and the total number of aircraft of type $i$. The variable $\mu_i(t)$ is the bank angle of aircraft type $i$ and denoted by $\mu_i(t) = \pm\tan^{-1}\left(\frac{V_{\mathrm{T},i}^2}{g_0 R}\right)$, where $V_{\mathrm{T},i}$ is the true airspeed of aircraft type $i$, $g_0$ is the gravitational acceleration, $R$ is the turn radius of the departure route, and $t$ is the time at the turns. The parameter $\mu_{\max}(h)$ is the maximum allowable value of $\mu$, which is stipulated for different altitudes $h$ by ICAO (2006). It should be noted that the calculation of $\mu_i(t)$ has been simplified based on the assumptions given in Section 3.2.

In the optimization problem in Eq. (1), the first objective $f_1(\mathbf{d})$ is the total number of people annoyed, which is evaluated based on a criterion defined within the European Union (EEA, 2010). According to EEA (2010), the percentage of people annoyed (%*PA*) caused by a certain $L_{\mathrm{den}}$ value, is determined as follows:

$$\%PA(\mathbf{r},\mathbf{d}) = 8.588\times10^{-6}(L_{\text{den}}(\mathbf{r},\mathbf{d})-37)^3 + 1.777\times10^{-2}(L_{\text{den}}(\mathbf{r},\mathbf{d})-37)^2 + 1.221\,(L_{\text{den}}(\mathbf{r},\mathbf{d})-37) \quad (2)$$

in which $L_{\text{den}}(\mathbf{r},\mathbf{d})$ is the day-evening-night noise level defined by

$$L_{\text{den}}(\mathbf{r},\mathbf{d}) = 10\log_{10}\left[\sum_{j=1}^{2}\sum_{i=1}^{N_{\text{at}}} a_{ij}10^{\frac{SEL_{ij}(\mathbf{r},\mathbf{d})+w_{\text{den}}}{10}}\right] - 10\log_{10}T\ (\text{dBA}), \quad (3)$$

where $\mathbf{r} = (x, y)$ is the vector of the center coordinates of a grid cell in the investigated area. The metric $SEL_{ij}(\mathbf{r},\mathbf{d})$ is the sound exposure level caused by aircraft type $i$ on route $j$ at the grid cells. This metric is calculated by employing a tool implemented in FORTRAN that uses an exact replication of the noise model described in the technical manual of the Integrated Noise Model (INM) (FAA, 2008). The parameters $w_{\text{den}} = \{0,5,10\}$ are the weighting factors for day, evening and night time operations. By using a Geographic Information System (GIS), the objective $f_1(\mathbf{d})$ can be determined by taking the sum of the multiplication of $\%PA$ in each grid cell with the population in that cell. The second objective $f_2(\mathbf{d})$ is the total fuel burn which aircraft consume during departure and is denoted as follows:

$$f_2(\mathbf{d}) = \sum_{j=1}^{2}\sum_{i=1}^{N_{\text{at}}} a_{ij}\, fuel_{ij}(\mathbf{d}), \quad (4)$$

where $fuel_{ij}(\mathbf{d})$ is the fuel burn of aircraft type $i$ on route $j$, which is evaluated based on the change of the aircraft weight during departure. The third objective $f_3(\mathbf{d})$ is a composite objective based on the Person Event Index (PEI), which is the number of noise events above 65 dBA $L_{\text{A,max}}(\mathbf{r},\mathbf{d})$ (so-called N65) multiplied by the population in each grid cell. Note that $L_{\text{A,max}}$ is also computed by using the same tool that is used to calculate $SEL_{ij}(\mathbf{r},\mathbf{d})$. It is recalled that the main objective is to distribute the noise impact whilst still minimizing the number of people annoyed as defined in objective $f_1(\mathbf{d})$. Thus, the third objective function is formulated as follows:

$$f_3(\mathbf{d}) = \sum_{j=1}^{2}\left(\bigcap_{i=1;\ \text{N65}}^{N_{\text{at}}} N_{\text{p},j}\sum_{i=1}^{N_{\text{at}}} a_{ij}k_j\right) + \sum_{j=1}^{2}\bigcap_{i=1;\ \text{N65}}^{N_{\text{at}}} S_{\text{p},j} \quad (5)$$

where the term $\bigcap_{i=1;\ \text{N65}}^{N_{\text{at}}} N_{\text{p},j}$ is the total number of people enclosed in the intersection of the N65 contours caused by all aircraft types on route $j$, while the term $\bigcap_{i=1;\ \text{N65}}^{N_{\text{at}}} S_{\text{p},j}$ is the total number of people enclosed in the intersection of N65 contours caused by all aircraft types on both routes. The parameter $k_j$ is a real number, which is equal to 1 if route $j$ accommodates more than or equal to 50% of the total aircraft movements, and 0 otherwise. It should be noted that the number of flights on each route is determined in advance for any individual aircraft type based on the information of the design variables of aircraft allocation, and hence the value $k_j$ in Eq. (5) is known.

In Eq. (5), the first component of the sum is essentially the PEI metric. Nevertheless, to avoid the trajectories converging at the same path, the PEI metric is only taken into account if the number of flights on a route is greater than or equal to 50%. This is controlled by the parameter $k_j$. Close to the runway, however, all departing aircraft still share the same ground track. People living in this area will be exposed to all aircraft movements regardless of the ground tracks of these routes or the allocation of flights to them. To ensure the trajectories are split up as soon as possible, and consequently to minimize the number of people exposed to all aircraft movements, the second component of Eq. (5) is taken into account. When minimized, this composite objective ensures that two distinct routes will be created that diverge as soon as possible within the limits of trajectory design and aircraft performance.

## 3. Trajectory parameterization and aircraft performance modeling

### *3.1. Trajectory parameterization*

In order to parameterize a trajectory in both the lateral and vertical plane, a trajectory parameterization technique developed recently by Hartjes and Visser (2016) is employed. This approach divides a trajectory into two isolated parts: a vertical path and a ground track. For the creation of the ground track, navigation based on required navigation performance (RNP) is assumed. In RNP, the flight path can be constructed by connecting waypoints through track-to-a-fix (TF) and radius-to-a-fix (RF) leg types. The advantages of using these leg types are that they can generate routes which can keep aircraft away from noise-sensitive areas and reduce flight track dispersion as well. Fig. 1 shows an example of a ground track generated using a sequence of TF and RF legs. From this figure, it can be observed that the design variable vector **g** of a departure route consisting of four straight legs and three turns comprises $L_1$, $L_2$, $L_{3,}$ $R_1$, $R_2$, $R_3$, $\Delta\chi_1$ and $\Delta\chi_2$, while $L_4$ and $\Delta\chi_3$ are determined through the geometric relationship assuming the initial and final position are fixed. In this work, two different routes with the same definition, i.e. the same number of leg types, are considered and optimized simultaneously. Therefore, the number of design variables for generating routes is doubled.

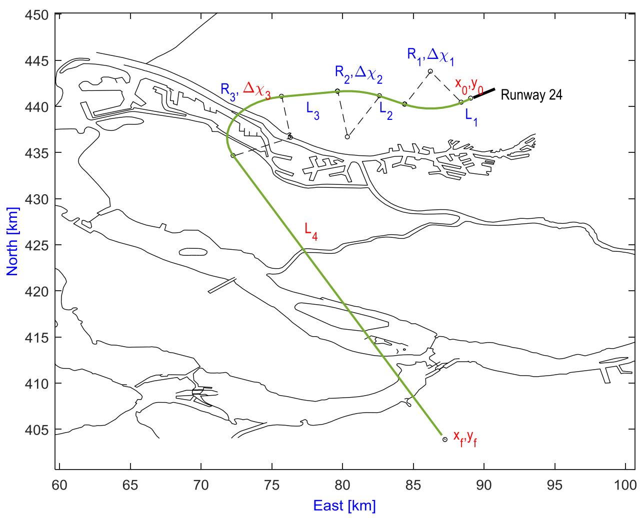


Fig. 1. Illustration of ground track parameterization.

For the vertical path, the vertical profile is created based on flight procedures derived from ICAO (2006), where two standard departure procedures, namely, Noise Abatement Departure Procedure 1 and 2 (NAPD1 and NADP2), as shown Fig. 2, are used. In this study, the vertical procedure is fixed and complies with either NAPD1 or NADP2. Therefore, there are no design variables considered in this part. Instead, the selection between NADP1 and NAPD2 is included as a design variable for each of the two routes. This aims to explore the advantage of these procedures for different routes as well as to ensure that the optimal routes can be applied to all aircraft types.

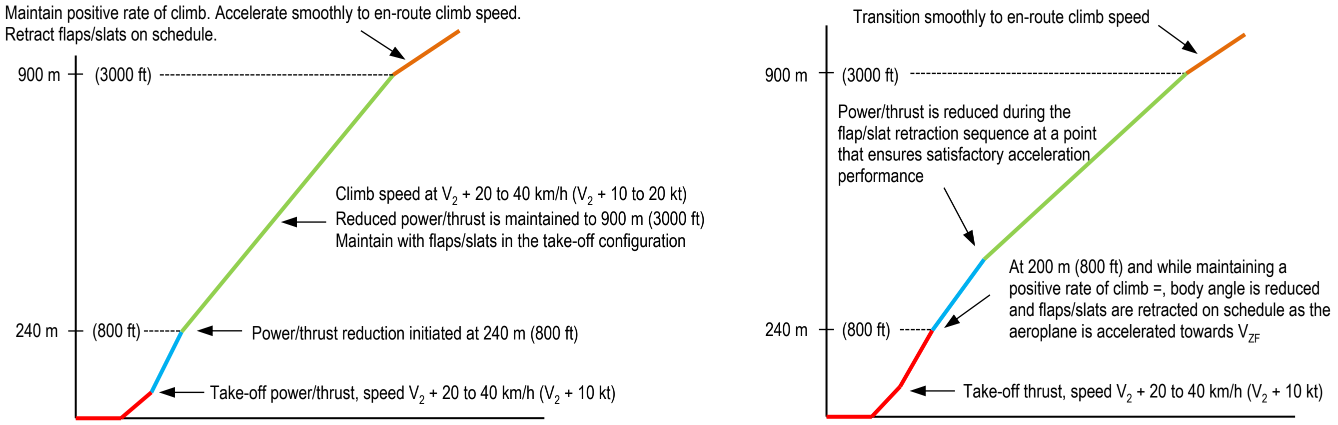


a) NADP1 b) NADP2

Fig. 2. Noise abatement departure procedure 1 and 2 (ICAO, 2006).

*3.2. Aircraft performance modeling*

In this study, an intermediate point-mass model is used (Hartjes and Visser, 2016). The model is based on some assumptions including: 1) no wind present, 2) a flat and non-rotating Earth, 3) coordinated flight, and 4) a sufficiently small flight path angle ($\gamma < 15^0$). With the given assumptions, the equations of motion can be written by

$$\begin{aligned} \dot{V}_\mathrm{T} &= g_0\left(\frac{T-D}{W}-\sin\gamma\right), \\ \dot{s} &= V_\mathrm{T}\cos\gamma, \\ \dot{h} &= V_\mathrm{T}\sin\gamma, \\ \dot{W} &= -ff\, g_0, \end{aligned} \tag{6}$$

in which, $V_\mathrm{T}, s, h$ and $W$ are the true airspeed, ground distance flown, altitude and aircraft weight, respectively. The parameters $T, D$ and $ff$ are, respectively, thrust, drag and fuel flow.

In case of low altitudes and airspeeds, the indicated airspeed can be approximated by the equivalent airspeed $V_\mathrm{E}$, and expressed as:

$$V_\mathrm{E} = V_\mathrm{T}\sqrt{\rho/\rho_0}, \tag{7}$$

where $\rho$ is the ambient air density, and $\rho_0$ is the air density at sea level.

Based on the relationship in Eq. (7), the equations of motion in Eq. (6) can be rewritten as follows:

$$\begin{aligned} \dot{V}_\mathrm{E} &= \left[g_0\left(\frac{T-D}{W}-\sin\gamma\right)+\frac{1}{2\rho^2}\frac{\partial\rho}{\partial h}V_\mathrm{E}^2\rho_0\sin\gamma\right]\sqrt{\rho/\rho_0}, \\ \dot{s} &= V_\mathrm{E}\sqrt{\rho_0/\rho}\cos\gamma, \\ \dot{h} &= V_\mathrm{E}\sqrt{\rho_0/\rho}\sin\gamma, \\ \dot{W} &= -ff\, g_0, \end{aligned} \tag{8}$$

where $\frac{\partial \rho}{\partial h}$ is the derivative of the ambient air density with respect to altitude.

By integrating Eq. (8) along the trajectory defined in Section 3.1, the input parameters for the calculation of *SEL* and $L_{A,max}$ are acquired. By using the tool to calculate noise, the values of $SEL_{ij}(\mathbf{r},\mathbf{d})$ and $L_{A,max}(\mathbf{r},\mathbf{d})$ at each grid cell are determined. When the velocity $V_T$, altitude $h$ and the geometry of the route are known, the bank angle constraints in Eq. (1) are also evaluated for each aircraft type.

## 4. Optimization algorithm

In this article, a new version of an optimization method called the multi-objective evolutionary algorithm based on decomposition (MOEA/D), which has been developed for the optimal design of departure routes in Ho-Huu et al. (2017) is employed. The method is a variant of the original MOEA/D algorithm proposed by Zhang and Li (2007), which has been demonstrated to be a potential candidate for solving complicated multi-objective optimization problems in the field of aerospace engineering (Ho-Huu et al. 2017). Therefore, it is again applied to solve the optimization problem stated in Section 2 in this study. However, compared with the problem in Ho-Huu et al. (2017), the considered optimization problem in this study is more complicated as it features three objectives and contains both continuous and discrete design variables, and equality constraints originating from the allocation of aircraft to different routes. To make the algorithm more efficient two techniques for handling these issues have also been developed. Since details of the algorithm have been given in Ho-Huu et al. (2017, 2018b) and Zhang and Li (2007), interested readers are encouraged to refer to these references, while the new techniques are presented in the next subsections.

### *4.1. Handling mixed discrete-continuous variables*

As pointed out in Section 2, the optimization problem has two different types of design variables, *viz.* continuous and discrete variables. The continuous variables are a set of geometric parameters to construct flight paths such as $L_1$, $L_2$, $R_1$, $R_2$, and $\Delta\chi_1$ as given in Section 3. The discrete variables are integer numbers, including the number of each aircraft type on each departure route, and variables to select between the two possible departure procedures (NADP1 or NADP2, which are labeled as 1 and 2, respectively). Since the original MOEA/D algorithm has been developed mainly for optimization problems with continuous design variables, to deal with these kinds of variables during the optimization process a simple rounding technique is applied to the set of discrete design variables. Specifically, whenever the optimization algorithm creates a new candidate for optimal solutions, all real-valued solutions indicated for discrete variables will be rounded to the nearest discrete values in their permissible sets, while there are no additional steps for the continuous variables. By applying this technique, it is ensured that all candidate solutions found by the algorithm satisfy the requirements of the optimization problem, and hence the unnecessary computational burden of infeasible solutions will be reduced significantly.

### *4.2. Handling equality constraints*

The MOEA/D algorithm is a population-based optimization method inspired by natural phenomena, finding optimal solutions by randomly searching with multi-design points at a time. Therefore, solving optimization problems by employing this method is often time-consuming. Recognizing this issue, in the recent version (Ho-Huu et al., 2017), we have developed a new adjustment on the settings of the optimization problem and the algorithm itself, which helps to significantly reduce the unnecessary computational cost. Compared to the original method, this variant has already shown to be very effective. However, this version only handles inequality constraints (i.e., bank angle constraints), while the problem considered in this study contains both inequality and equality constraints. As seen in Eq. (1), the equality constraint ensures that the number of aircraft allocated to the two alternative departure routes must be equal to the total number of aircraft. However, it is obvious that many solutions created by the algorithm do not satisfy all constraints – especially the equality constraints. Consequently, if we approach this problem by using typical methods for constraint handling like the penalty method, the computational cost spent on the evaluation of infeasible solutions will be extremely high. Therefore, while keeping the same technique for coping with the inequality constraints as in the previous version, a new simple technique for handling equality constraints is introduced in this work.

A general procedure of the technique is presented in steps as follows:

- In the optimization problem in Eq. (1), each equality constraint $i$ ($i$ = 1,…, $N_{at}$) is replaced by a new variable $c_i$.
- For each new variable $c_i$, the set of feasible combinations $\mathbf{S}_i$ of the allocation of aircraft type $i$ to all routes is defined. Note that a combination is feasible when the sum of the number of aircraft on all routes is equal to the total number of aircraft type $i$ ($\mathrm{T}_{at,i}$).
- In set $\mathbf{S}_i$, the combinations are represented by integer values, which are numbered from 1 to the last combination. Then, the design space as well as the boundaries of variables $c_i$ are determined, which are integer values. The lower bound is set to 1, and the upper bound will be the length of set $\mathbf{S}_i$.

In order to make the proposed approach more transparent, a simple example is considered here. It is assumed that there are 20 flights with only one aircraft type which need to be distributed over two departure routes. From Eq. (1), we have $i$ = 1, $j$ = 2, and the equality constraint is defined as $a_{11} + a_{12} = 20,$ with $a_{11}, a_{12} \in \{0,1,2,...,20\}$. From this constraint, it is obvious that there is only a set of twenty-one possible combinations between $a_{11}$ and $a_{12}$ which satisfy the constraint, $\mathbf{S}$ = $\{\{0,20\},\{1,19\},\ldots,\{10,10\},\ldots,\{19,1\},\{20,0\}\}$. This set can be represented by defining a new variable $c$ ($c \in \{1,2,...,21\}$), where 1, 2, …, 21 are, respectively, the combinations of {0,20}, {1,19}, …, {20,0}. In addition, in this work the design of two alternative routes and the allocation of aircraft movements take place simultaneously and flexibly, hence the set of $\mathbf{S}$ can be reduced from twenty-one to eleven combinations and denoted by $\mathbf{S}$ = $\{\{0,20\},\{1,19\},\ldots,\{10,10\}\}$. Consequently, the search space of the variable $c$ is decreased considerably. It should be noted that for this specific example – having only two design variables in the equality constraints – we can use only $a_{11}$ as a design variable, and $a_{12}$ can be derived from the definition of the equality constraint. This approach is, however, only valid for equality constraints with two design variables. In addition, it should be noted that the proposed technique may be limited for certain problems with limited numbers of design variables as the set of feasible combinations will increase significantly with larger numbers of design variables.

In summary, applying the above technique to all equality constraints for the aircraft allocation will help decrease the complexity of the optimization problem and reduce the search space of the problem. Hence, the optimization process will be much faster, and the computational cost can be diminished considerably.

## 5. Numerical results and discussions

To demonstrate the reliability and applicability of the proposed approach, two different case studies are carried out in this section. The first example is a scenario at Rotterdam The Hague Airport (RTM), where a standard instrument departure (SID) named WOODY is considered. The second example is set at Amsterdam Airport Schiphol (AAS), where a SID called LUNIX is investigated. In order to evaluate the influence of the third objective on the optimal routes, for each case study two different optimization problems are evaluated. In the first problem only the two objectives $f_1(\mathbf{d})$ and $f_2(\mathbf{d})$ are optimized, while the second problem considers all three objectives at the same time. Both SIDs are currently in use at the airports, and the existing SIDs are used as reference solutions in the next sections. To solve the optimization problems, the MOEA/D algorithm is used with a population size of 50 and a maximum number of iterations of 1000. The search process of the algorithm will be terminated when either the stopping criterion is met or the maximum number of iterations has been reached. All simulations are implemented in Matlab 2016b on an Intel Core i5, 8GB RAM desktop.

### *5.1. Rotterdam The Hague Airport case study*

Rotterdam The Hague Airport is a regional airport located to the north of the city of Rotterdam in The Netherlands, and is surrounded by densely populated regions such as The Hague, Rotterdam, and Utrecht. The design of a new optimal departure route for the WOODY SID, in this example, is assumed to start at the end of runway 24 at an altitude of 35 ft and a take-off safety speed of $V_2$+10 kts, and finishes at waypoint EH162 at an altitude of 6,000 ft and an equivalent airspeed (EAS) of 250 kts. It is assumed that on a peak day, there are 40 flights following this SID. This assumption is based on the reference data at flightradar24[**] in the summer season, which also indicates that there are only three aircraft types commonly operating from RTM, *viz.* the Embraer 190 (E190), Boeing 737-700 (B737) and B737-800 (B738). Also, in an effort to avoid the noise computation burden associated with the noise impact assessment, these aircraft can be represented by one aircraft type (Hartjes et al., 2014). In this study, the B738 is selected as a representative aircraft for the noise calculations. It is also noted that for the allocation of aircraft, the real departure times are ignored, and hence all flights are assumed to count as a day-time flight in the determination of the noise impact.

By applying the parameterization technique described in Section 3 and allocation variables described in Section 4.2, the optimization problems have nineteen design variables: sixteen variables to describe the two alternative ground tracks, one for the aircraft allocation, and one to select the departure procedures. An area of 22×30.5 km and a population grid cell size of 500×500 m (based on data obtained from the Dutch Central Bureau of Statistics (CBS)) are used for the noise calculations, as shown in Fig. 3. The aircraft are modeled based on the Base of Aircraft Data (BADA) (Angela et

[**] https://www.flightradar24.com/data/airports/rtm/departures

al., 2010). The optimization takes 3.08 hours (h) with 562 interations and 4.31 h with 942 iterations to achieve a full convergence for the first and second problems, respectively.

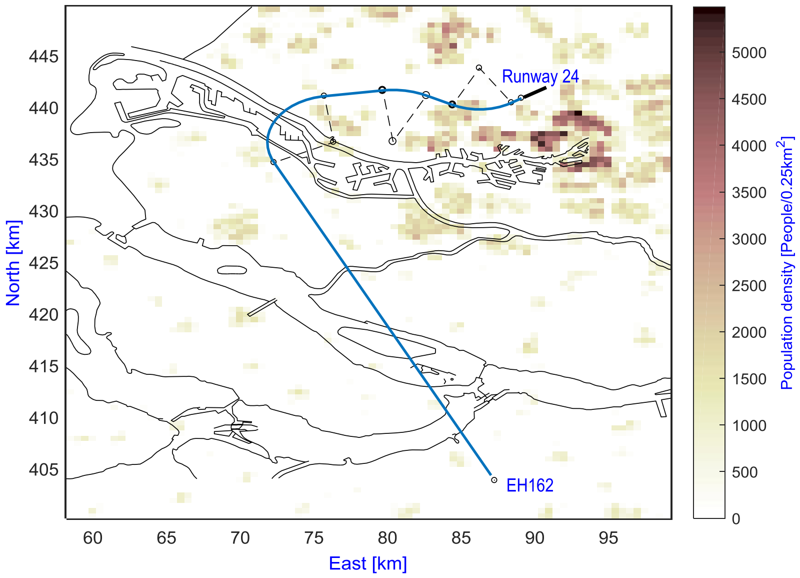


Fig. 3. Departure route WOODY.

The comparison of Pareto solutions for fuel burn and number of people annoyed obtained by both approaches are presented in Fig. 4, in which the reference solutions are marked as well. The Pareto solutions acquired by solving the second problem (optimization with three objectives) are given in Fig. 5. As seen in Fig. 4, the solutions acquired by both approaches are quite close, and most of the solutions obtained by the first approach dominate those of the second one. Nevertheless, if the third objective (essentially representing the spreading of the noise impact) is considered to evaluate the results of the first approach, all of their solutions are worse than those of the second approach. This is because the solutions obtained by the second approach have to balance between the three objectives, while those of the first problem only balance between the first two objectives. Moreover, as shown in Fig. 4, the second approach can also provide some solutions which dominate some of the solutions found in the first problem. In a comparison with the reference solution, from the figure, it is observed that both approaches offer better solutions regarding both fuel burn and number of annoyed people.

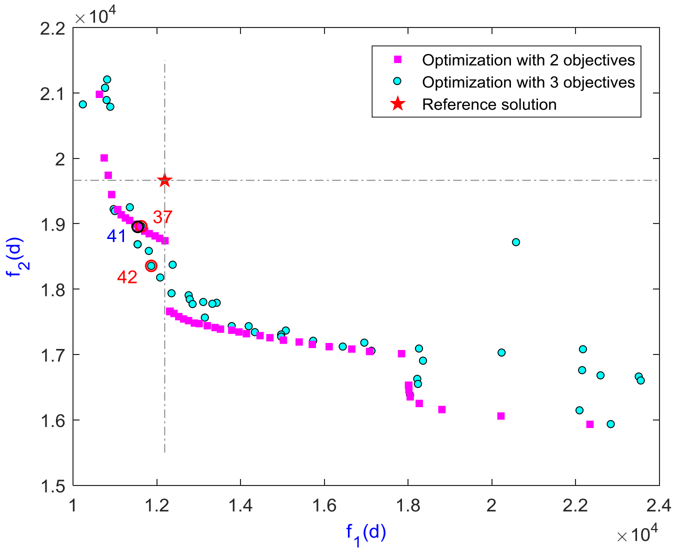


Fig. 4. Comparison of Pareto fronts obtained by the first and second problems and the reference case.

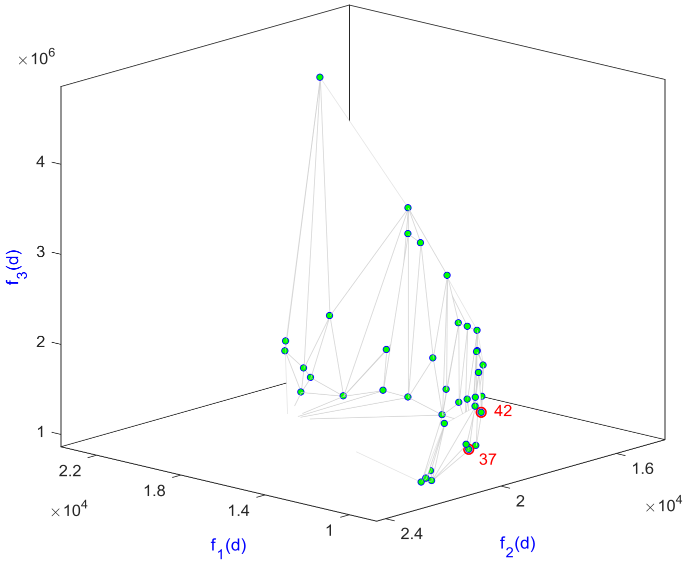


Fig. 5. Pareto fronts obtained by the second problem.

The ground tracks corresponding to the solutions given in Fig. 4 and Fig. 5 are provided in Fig. 6 and Fig. 7, where the former shows those of the first problem, and the latter shows those of the second one. Some routes have been highlighted corresponding to the solutions highlighted in Fig. 4 and Fig. 5. It should be noted that in all results the NADP2 departure procedure is selected as an optimal procedure for all obtained routes. For the first approach – only considering fuel burn and people annoyed – only one optimal route is found for each solution, and all aircraft are allocated on the same route as can be seen in Fig. 6. On the other hand, when considering all three objectives, most of the solutions contain two distinct routes with different allocations of aircraft as shown in Fig. 7, where the alternative routes are indicated by solid and dashed lines. Looking at the figures, it can be seen that all the solutions tend to avoid the most densely populated areas.

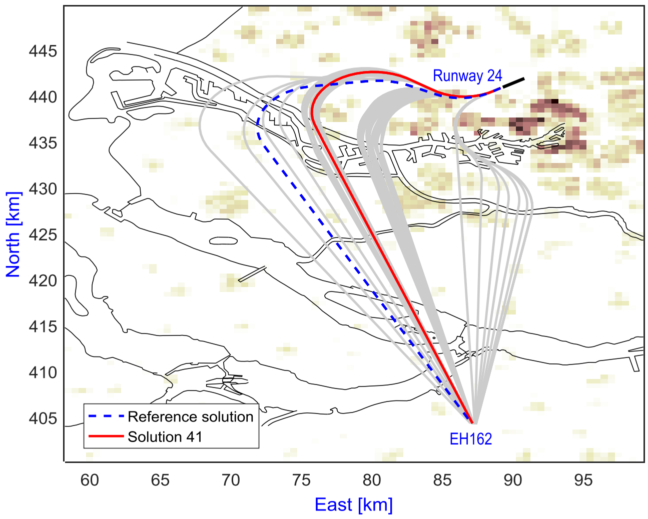


Fig. 6. Optimal ground tracks obtained in the first problem.

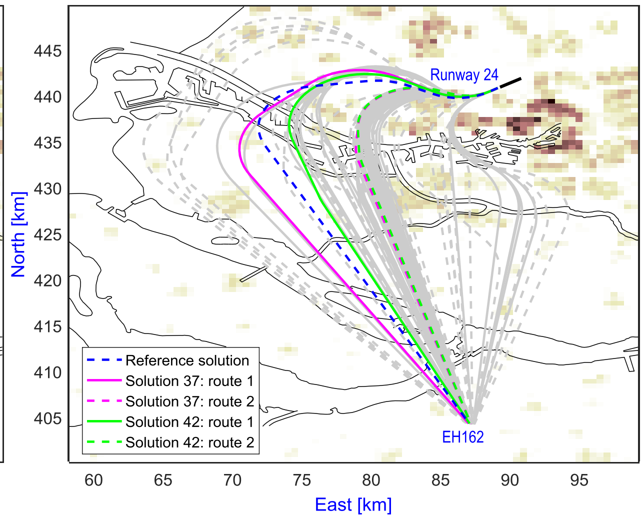


Fig. 7. Optimal ground tracks obtained in the second problem.

In order to show the comparison between the two different approaches and the reference case more clearly, the ground tracks of the representative solutions as highlighted in Fig. 4, and that of the reference solution, are presented in Fig. 8, where the N65 and 37 dBA $L_{den}$ contours the threshold level for annoyance) are given as well. A comparison of the representative solution 41 of the first problem with the reference case indicates that route 41 takes a longer initial right turn to avoid the population close to the runway and turns towards the South sooner to reduce the total ground distance and hence the fuel burn. Therefore, its performance is better than the reference case for both objectives. Similarly, solutions 37 and 42 of the second approach show the same trend. Looking at solution 37, though the first route (red line) is longer than the reference route, the second one is much shorter, and owing to the distinct distribution of aircraft on each route (19 flights on the red route and 21 flights on the blue route), the total fuel burn is reduced significantly. This is similar for solution 42. Nevertheless, due to the spreading of the noise, the $L_{\text{den}}$ contours of these solutions are larger than those of solution 41 and the reference solution, which may lead to a higher number of people annoyed. The numerical results presented in Table 1, however, show that the number of people annoyed has not significantly increased as compared to solution 41 optimized for only two objectives. The explanation for this can be seen in Fig. 9, where it can be seen that although the 37 dBA $L_{\text{den}}$ contours are wider, the concentration of noise is lower, which limits the increase in the number of annoyed people as compared to solution 1. For the third objective, representing the spreading of noise, however, solutions 37 and 42 obviously provide a considerable reduction, while for the reference case and solution 41, this objective logically remains very high. In addition, the conflicting nature of the considered objectives can also be observed in these figures. While the conflict of the first two objectives is quite apparent in Fig. 4, the potential conflict between them and the third objective can be recognized in the comparison of solution 41 and solutions 37 and 42, as shown in Fig. 8. More specifically, in the case where all aircraft follow the same route as in solution 41, it is obvious that the number of annoyed people is reduced significantly owing to the narrow $L_{\text{den}}$ contour. Nevertheless, all people living underneath the flight path will be exposed to all aircraft movements. Meanwhile, if there is a sharing of routes as in solutions 37 and 42, the number of annoyed people will be higher, but the number of people exposed to all flights is significantly lower. Based on these observations, it can be concluded that the optimization problem formulated in Section 2 is reasonable and basically satisfies the general requirements of a multi-objective optimization problem. From a practical point of view, however, it should be noted that since the distribution of optimal routes depends highly on the distribution of population around the airport, in some cases these objectives may or may not conflict.

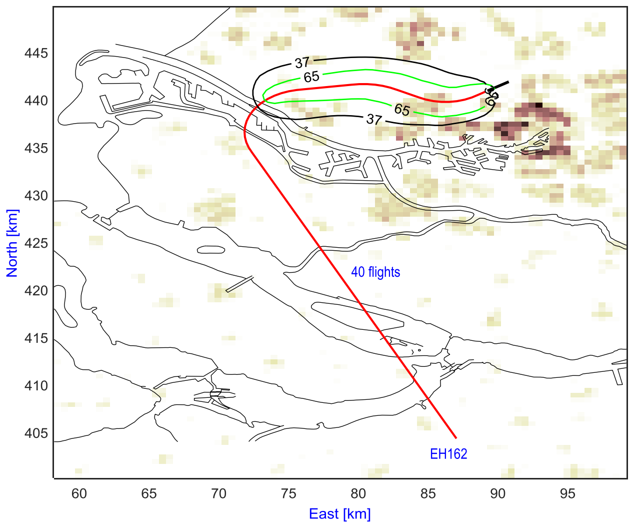

a) Reference solution

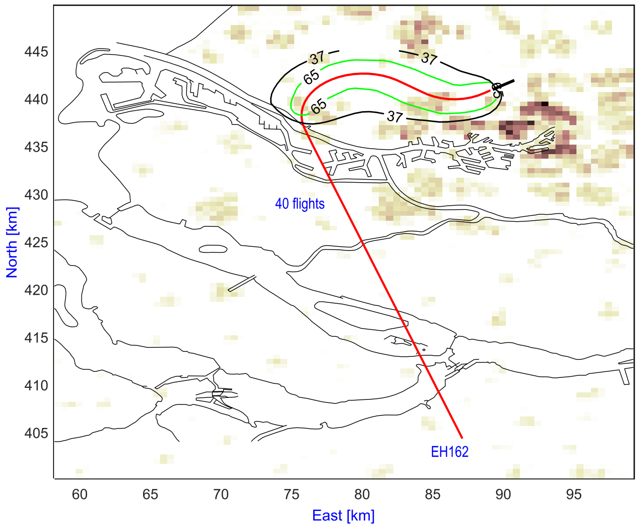

b) Solution 41

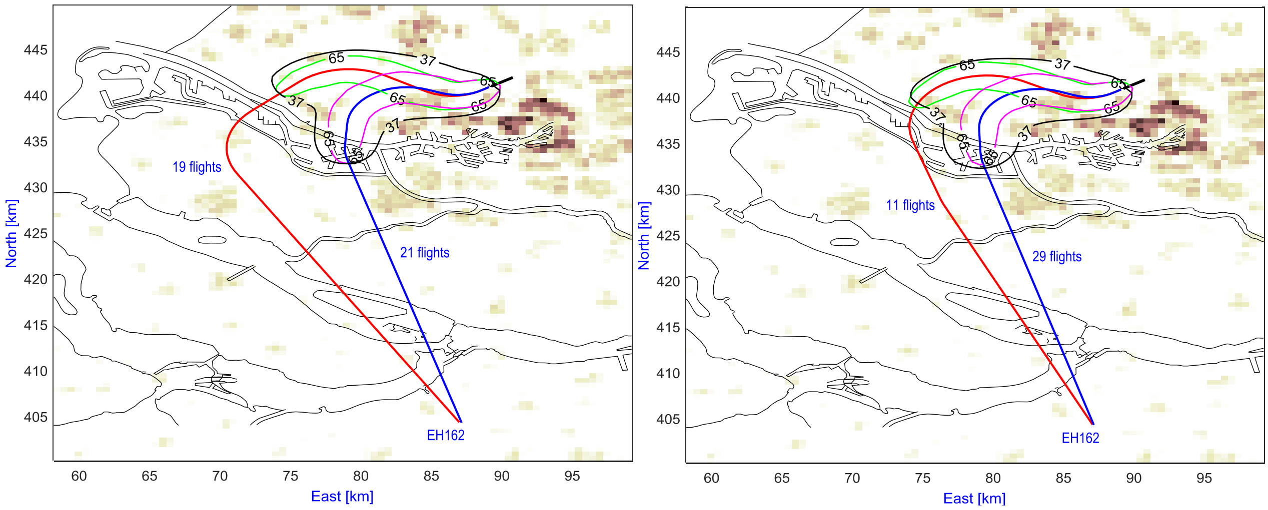


c) Solution 37 d) Solution 42

Fig. 8. Illustration of $L_{\mathrm{den}}$ and N65 contours of the representative routes and the reference case.

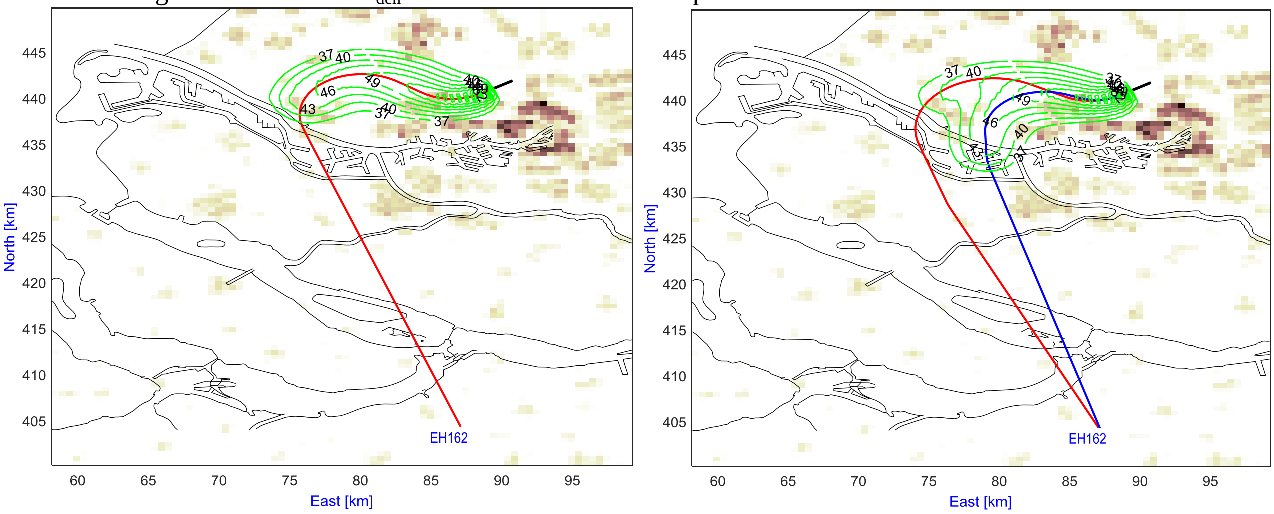


c) Solution 41 d) Solution 42

Fig. 9. Illustration of the concentration of $L_{\mathrm{den}}$ contours of solutions 41 and 42.

The specific comparison of indicators estimated by the representative and reference cases is given in Table 1. The indicators contain number of people annoyed, fuel burn, number of people enclosed in the N65 contour and exposed more than 50% of the flights, the Person Event Index (PEI), and the Average Individual exposure (AIE) (which is the division of PEI and the total exposed population). At first glance, compared with the reference solution, all the metrics obtained by solutions 37 and 42 are better, while solution 41 only performs better at two metrics and equal or worse in the other three metrics. Regarding the number of annoyed people, it can be seen from the table that solution 41 gives the best reduction of 5.8% with respect to the reference case, while those of solutions 37 and 42 obtain 4.5% and 2.5%, respectively. In contrast, solutions 42 and 37 outperform solution 41 for all other metrics. More specifically, solutions 42 and 37 result in a decrease of 6.7% and 3.6% in fuel burn, respectively, while that of solution 41 is only 3.4%. In terms of the number of people living within the N65 contour and exposed to more than 50% of all flights, solutions 42 and 37 yield a good reduction of 7.4% and 5.5%, respectively, whereas solution 41 results in a significant increase of 10.9% compared to the reference case. Similarly, the comparison of the PEI also shows the same trend, in which the PEI of solution 41 increases with 10.9%, while that of solutions 37 and 42 reduces by 7.6%

and 6.1%, respectively. Finally, regarding the AIE metric, only those obtained by solutions 37 and 42 show a reduction of 19.2% and 15.3%, respectively.

Table 1. Comparison of the metrics of the representative solutions and the reference case.

| Optimization approaches | Case number | No. of people annoyed | Fuel burn (kg) | No. of people living within N65 and exposed ≥ 50% of flights | PEI (Person Event Index) | AIE (Average Individual Exposure) |
|---|---|---|---|---|---|---|
| 2 objectives | Solution 41 | 11476 | 18993 | 54340 | 2173600 | 40 |
| | *% reduction* | -5.8 | -3.4 | +10.9 | +10.9 | 0.0 |
| 3 objectives | Solution 37 | 11642 | 18952 | 46295 | 1811140 | 34 |
| | *% reduction* | -4.5 | -3.6 | -5.5 | -7.6 | -15.3 |
| | Solution 42 | 11879 | 18347 | 45385 | 1840865 | 32 |
| | *% reduction* | -2.5 | -6.7 | -7.4 | -6.1 | -19.2 |
| Reference solution | | 12189 | 19664 | 49000 | 1960000 | 40 |

In summary, based on the obtained results, it can be concluded that the proposed approach using three objectives can provide new optimal routes which result in a better spread of the noise impact, while still performing almost as good as routes optimized for more traditional noise impact criteria such as annoyance.

### *5.2. Amsterdam Schiphol Airport case study*

In order to further evaluate the performance of the proposed approach, a case study at Amsterdam Schiphol Airport in The Netherlands is considered as well. The airport is an international airport and one of the busiest airports in the world, and is located to the southwest of the city of Amsterdam. In this example, the SID named LUNIX is investigated. The trajectory starts at the end of runway 24 and ends at the IVLUT intersection. The initial and final airspeed and altitudes are the same as in the previous case. Regarding the number of flights and aircraft types, it is assumed that there are 400 flights operating on this SID on a busy day with a highly diverse fleet mix. For this example, it is assumed that the fleet mix consists of 80% medium aircraft represented by the B738 and 20% heavy aircraft represented by the Boeing 777-300 (B773). As in the case study at RTM, the actual departure times of flights are ignored.

This optimization problem has fourteen design variables: ten to define the routes, two for the allocation of flights and two to select the departure procedure. An area of 51.5×23 km and a population grid cell size of 500×500 m as shown in Fig. 10 are used. To solve the optimization problems, the algorithm converges after 652 iterations in 9.18 h and 912 iterations in 12.06 h for the first and second problems, respectively. It should be noted that, compared with the previous example, the significant increase in the computational cost in this problem is due to the consideration of two differernt aircraft types at the same time. Moreover, the investigated area in this example is also larger than the area considered in the previous example.

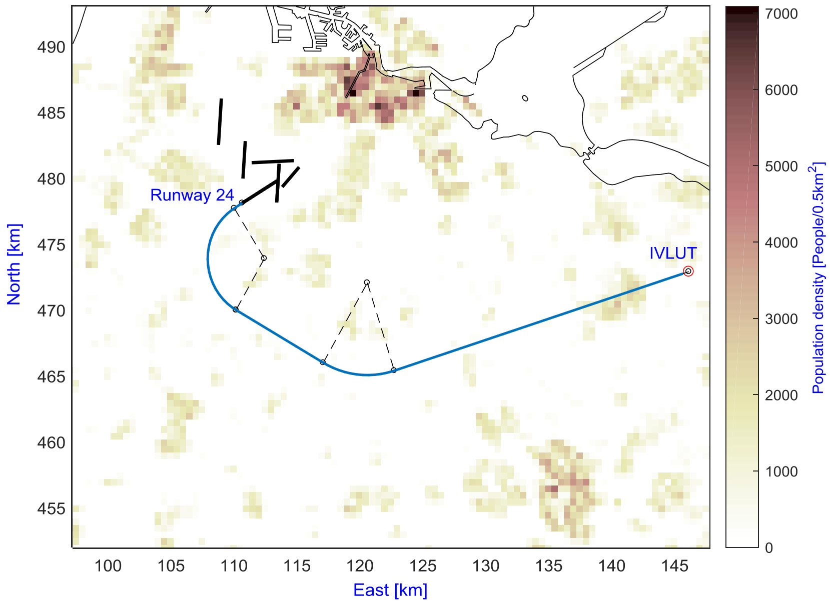


Fig. 10. Departure route LUNIX.

Fig. 11 shows the comparison of Pareto solutions with the reference case for fuel burn and number of annoyed people obtained by both approaches. The Pareto solutions gained by solving the optimization problem with three objectives (the second problem) are presented in Fig. 12. It can be seen in Fig. 12 that some solutions of the second approach are located on the Pareto front resulting from the bi-objective optimization. In these solutions, the first two objectives are dominant, and in fact these solutions share a common ground track rather than two alternative routes, resulting in a high value for the third objective. The figure also shows that some solutions (from both approaches) dominate the reference case. However, these solutions again only have one common route, and hence they perform very poorly with respect to the third objective. In an effort to identify solutions which are good at distributing the noise impact over different communities while not significantly compromising the other two objectives, solutions 42 and 49 of the second approach are further evaluated as representative cases. Furthermore, to provide an alternative choice disregarding the third objective, solution 27 of the first approach, which dominates the reference case, is also selected for evaluation.

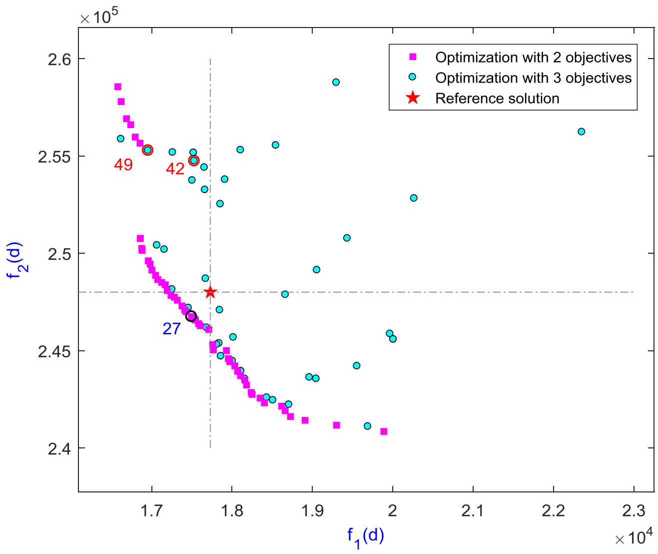


Fig. 11. Comparison of Pareto fronts obtained by the first and second problems and the reference case.

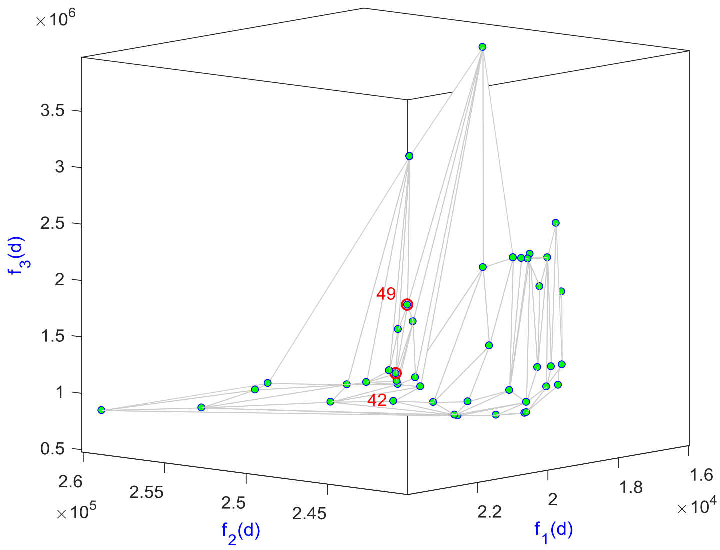


Fig. 12. Pareto fronts obtained by the second problem.

The ground tracks of the solutions obtained by the two approaches are shown in Fig. 13 and Fig. 14, respectively. From the figures, it can be seen that in all solutions noise-sensitive areas are avoided. Again, NADP2 is selected as the optimal departure procedure for all ground tracks and all aircraft types in both approaches. For the first problem, only one optimal route is found for each solution, and all aircraft follow the same route. On the other hand, the second approach comprises both kinds of solutions which have either one route or two different routes.

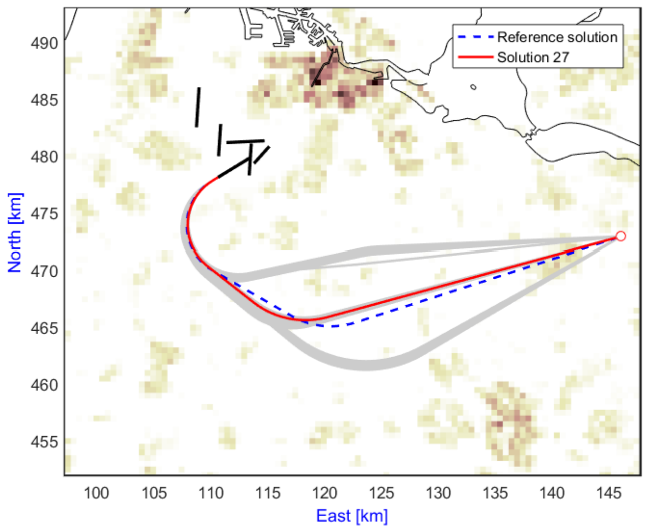


Fig. 13. Optimal ground tracks obtained by the first problem.

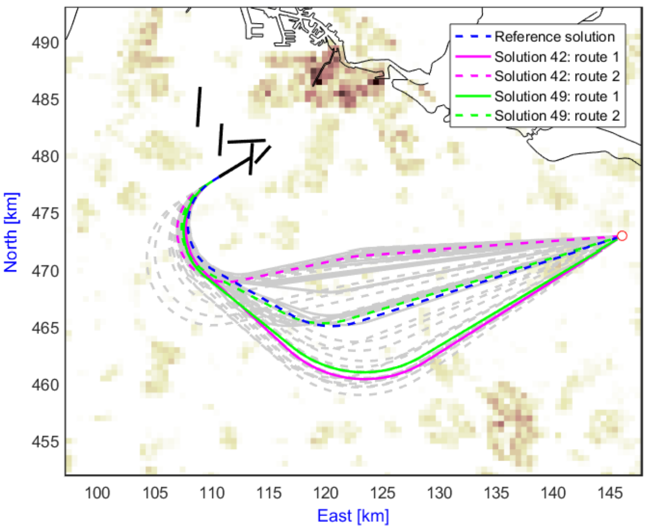


Fig. 14. Optimal ground tracks obtained in the second problem.

To make the comparison more explicit, the ground tracks of the representative solutions and that of the reference case are isolated in Fig. 15, in which again the 37 dBA $L_{den}$ and N65 contours (B738 in magenta and B773 in green) are provided. As can be seen in the figure, compared to the reference case, solutions 42 and 49 have two distinct routes, while solution 27 has only one route. Regardless of the share of aircraft noise, it can be seen that the number of people living within the N65 contour and exposed to more than 50% of all flights obtained by solutions 42 and 49 is reduced significantly compared with those of solution 27 and the reference case. This can be seen in the numerical results in Table 2 as well.

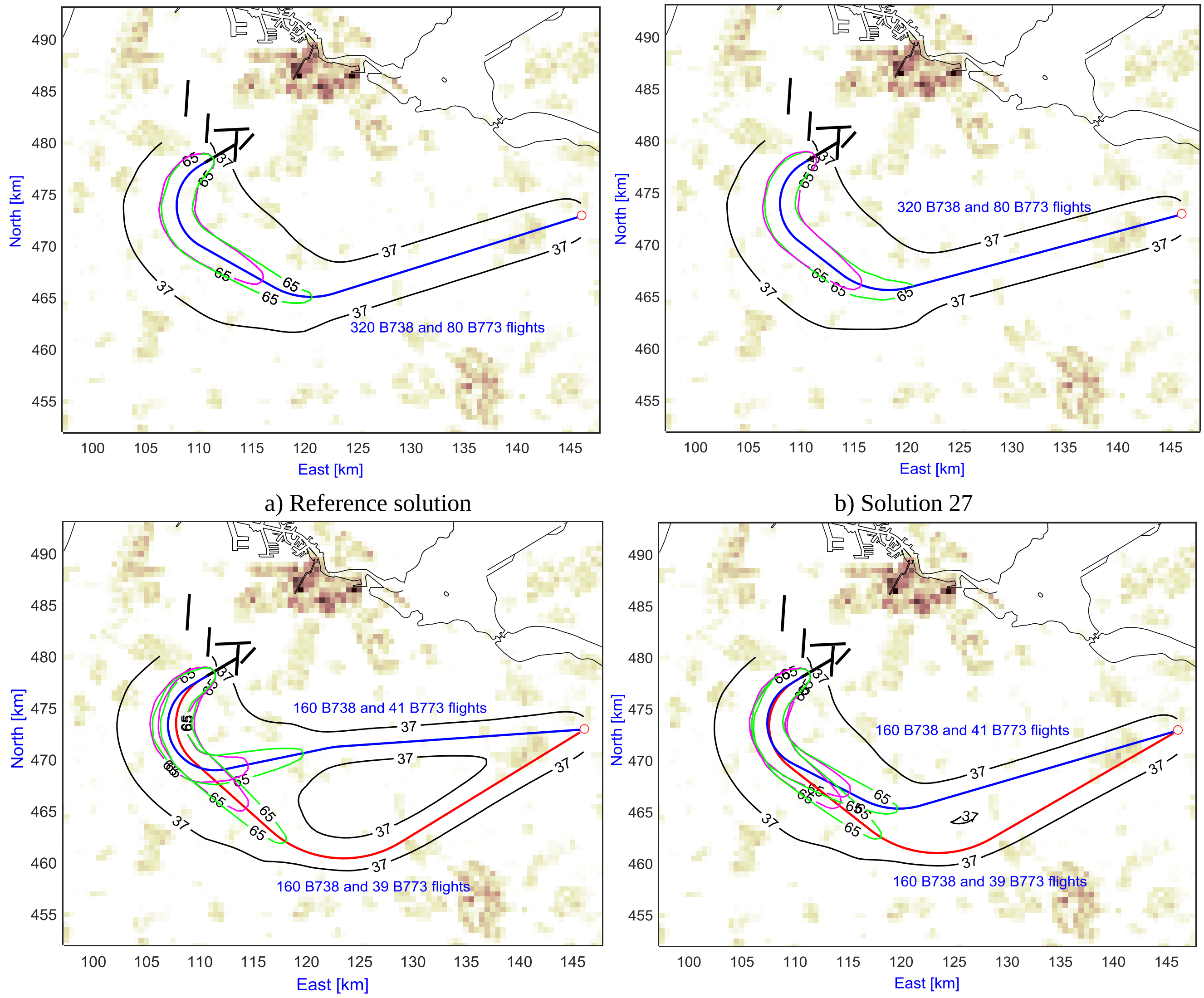


a) Reference solution

b) Solution 27

c) Solution 42

d) Solution 49

Fig. 15. Illustration of $L_{\mathrm{den}}$ and N65 contours of the representative routes and the reference case.

The table also shows that the three representative solutions show a small improvement in terms of the number of people annoyed, and a slight increase in fuel burn as compared to the reference case. However, especially solution 42 shows a large reduction in the third objective, indicating that the noise load – which is already slightly lower for the more traditional annoyance criterion – is spread out much better over different communities, indicating that the individual annoyance related to frequency could be lowered significantly.

Table 2. Comparison of the metrics of the representative solutions and the reference case.

| Optimization approaches | Case number | No. of people annoyed | Fuel burn (kg) | No. of people living within N65 and exposed ≥ 50% of flights | PEI (Person Event Index) | AIE (Average Individual Exposure) |
|---|---|---|---|---|---|---|
| 2 objectives | Solution 27 | 17496 | 246749 | 9785 | 4031600 | 340 |
| | *% reduction* | -1.3 | -0.5 | +19.5 | +19.7 | +0.7 |
| 3 objectives | Solution 42 | 17531 | 254740 | 4575 | 3420575 | 233 |
| | *% reduction* | -1.1 | +2.7 | -44.1 | +1.6 | -31.1 |

| | | | | | |
|---|---|---|---|---|---|
| Solution 49 | 16956 | 255278 | 7380 | 3768615 | 293 |
| *% reduction* | -4.4 | +2.9 | -9.8 | +11.9 | -13.4 |
| Reference solution | 17729 | 248006 | 8185 | 3367200 | 338 |

In summary, the method discussed above shows potential to reduce the annoyance whilst at the same time improving the distribution of the noise load over different communities, at the cost of only a minor increase in the ground path length.

## 6. Conclusion

In an effort to effectively balance the concerns regarding the environmental impacts caused by aircraft and airport operations, a new formulation for the design of optimal departure routes and the allocation of flights to these routes has been developed in this paper. Apart from two conventional objectives, as a novel feature, a new objective has been developed and included in the optimization problem. This objective aims to take into account the frequency of noise events for individual people, and in essence ensures a fairer distribution of the noise impact over the communities surrounding an airport. In order to take advantage of the combination of designing new routes and allocating flights to these routes, two different routes have been considered, and the distribution of flights on these two routes is optimized simultaneously. Also, to solve the optimization problem, a new version of the MOEA/D algorithm has been developed, in which a new technique for handling equality constraints and a simple technique for dealing with mixed continuous-discrete design variables have been introduced. The reliability and applicability of the proposed approach are exemplified through two different case studies at Rotterdam The Hague Airport and at Amsterdam Airport Schiphol in The Netherlands. The obtained simulation results reveal that the proposed approach can provide solutions in which the fair distribution of the noise impact has improved significantly, whilst the traditional noise impact criterion based on annoyance is increasing only slightly or – in some cases – decreasing as compared to the reference case based on current-day operations.

However, the work presented in this paper has also led to the identification of further challenges. Firstly, the developed fairness metric relies on the assumption that the frequency of noise events is indeed a concern. Consequently, more research would be needed to identify the impact of exposure frequency on annoyance. In addition, by applying this approach each SID will have (at least) two different routes which may cause operational challenges and may increase the workload of air traffic controllers. Though this study is based on representative amounts of aircraft movements and hence departure capacity itself should not be an issue, the merging of two or more alternative routes at the final point may also negatively affect the controller's workload. Therefore, these problems should be considered in the future.

## References

Angela, N., Damir, P., Vincent, M., 2010. BADA: An advanced aircraft performance model for present and future ATM systems. Int. J. Adapt. Control Signal Process. 24, 850–866. doi:10.1002/acs.1176

ANSI/ASA, 2008. Quantities and Procedures for Description and Measurement of Environmental Sound - Part 6: Methods for Estimation of Awakenings Associated with Outdoor Noise Events Heard in Homes.

Boeing, 2016. Current Market Outlook 2016–2035.

Braakenburg, M.L., Hartjes, S., Visser, H.G., 2011. Development of a Multi-Event Trajectory Optimization Tool for Noise-Optimized Approach Route Design. AIAA J. 1–13. doi:10.2514/6.2011-6929

Brown, A.L., 2014. An overview of concepts and past findings on noise events and human response to surface

transport noise, in: Internoise 2014. 16-19 November, Melbourn, Australia, pp. 1–8.
Department of Transport and Regional Services, 2000. Expanding Ways to Describe and Assess Aircraft Noise.
European Environment Agency (EEA), 2010. Good practice guide on noise exposure and potential health effects, in: EEA Technical Report.
Federal Aviation Administration (FAA), Office of Environment and Energy, 2008. INM User's Guide, Integrated Noise Model, INM 7.0, Technical Manual, FAA-AEE- 08-01.
Federal Interagency Committee on Aviation Noise (FICAN), 1997. Effects of aviation noise on awakenings from sleep.
Fields, J.M., 1984. The effect of numbers of noise events on people's reactions to noise: An analysis of existing survey data. J. Acoust. Soc. Am. 75, 447–467. doi:10.1121/1.390469
Frair, L., 1984. Airport noise modelling and aircraft scheduling so as to minimize community annoyance. Appl. Math. Model. 8, 271–281. doi:https://doi.org/10.1016/0307-904X(84)90162-8
Green, J.E., 2005. Air Travel – Greener by Design Mitigating the environmental impact of aviation: Opportunities and priorities. Aeronaut. J. 109, 361–416. doi:10.1017/S0001924000000841
Hartjes, S., Dons, J., Visser, H.G., 2014. Optimization of Area Navigation Arrival Routes for Cumulative Noise Exposure. J. Aircr. 51, 1432–1438. doi:10.2514/1.C032302
Hartjes, S., Visser, H., 2016. Efficient trajectory parameterization for environmental optimization of departure flight paths using a genetic algorithm. Proc. Inst. Mech. Eng. Part G J. Aerosp. Eng. 0, 1–9. doi:10.1177/0954410016648980
Hartjes, S., Visser, H.G., Hebly, S.J., 2010. Optimisation of RNAV noise and emission abatement standard instrument departures. Aeronaut. J. 114, 757–767. doi:10.1017/CBO9781107415324.004
Ho-Huu, V., Hartjes, S., Geijselaers, L.H., Visser, H.G., Curran, R., 2018a. Optimization of noise abatement aircraft terminal routes using a multi-objective evolutionary algorithm based on decomposition. Transp. Res. Procedia 29, 157–168. doi:10.1016/j.trpro.2018.02.014
Ho-Huu, V., Hartjes, S., Visser, H., Curran, R., 2017. An Efficient Application of the MOEA/D Algorithm for Designing Noise Abatement Departure Trajectories. Aerospace 4, 54. doi:10.3390/aerospace4040054
Ho-Huu, V., Hartjes, S., Visser, H.G., Curran, R., 2018b. An improved MOEA / D algorithm for bi-objective optimization problems with complex Pareto fronts and its application to structural optimization. Expert Syst. Appl. 92, 430–446. doi:10.1016/j.eswa.2017.09.051
Hogenhuis, R.H., Hebly, S.J., Visser, H.G., 2011. Optimization of area navigation noise abatement approach trajectories. Proc. Inst. Mech. Eng. Part G-Journal Aerosp. Eng. 225, 513–521. doi:10.1177/09544100JAERO840
International Civil Aviation Organization (ICAO), 2006. Procedures for air navigation services – Aircraft operations. Vol. I, Flight Procedures.
Janssen, S.A., Centen, M.R., Vos, H., Van Kamp, I., 2014. The effect of the number of aircraft noise events on sleep quality. Appl. Acoust. 84, 9–16. doi:10.1016/j.apacoust.2014.04.002
Khardi, S., Abdallah, L., 2012. Optimization approaches of aircraft flight path reducing noise: Comparison of modeling methods. Appl. Acoust. 73, 291–301. doi:10.1016/j.apacoust.2011.06.012
Kim, B., Li, L., Clarke, J.-P., 2014. Runway Assignments That Minimize Terminal Airspace and Airport Surface Emissions. J. Guid. Control. Dyn. 37, 789–798. doi:10.2514/1.61829
Kuiper, B.R., Visser, H.G., Heblij, S., 2012. Efficient use of an allotted airport annual noise budget through minimax optimization of runway allocations. Proc. Inst. Mech. Eng. Part G J. Aerosp. Eng. 227, 1021–1035. doi:10.1177/0954410012447767
Marais, K.B., Reynolds, T.G., Uday, P., Muller, D., Lovegren, J., Dumont, J.-M., Hansman, R.J., 2013. Evaluation of potential near-term operational changes to mitigate environmental impacts of aviation. Proc. Inst. Mech. Eng. Part G J. Aerosp. Eng. 227, 1277–1299. doi:10.1177/0954410012454095
Porter, N., Knowles, A., Fisher, N., Southgate, D., 2014. The next generation of supplementary aviation noise metrics and their use in managing aviation noise ., in: Internoise 2014. 16-19 November, Melbourn, Australia, pp. 1–10.
Prats, X., Puig, V., Quevedo, J., 2011. Equitable Aircraft Noise-Abatement Departure Procedures. J. Guid. Control. Dyn. 34, 192–203. doi:10.2514/1.49530
Prats, X., Puig, V., Quevedo, J., Nejjari, F., 2010a. Lexicographic optimisation for optimal departure aircraft trajectories. Aerosp. Sci. Technol. 14, 26–37. doi:10.1016/j.ast.2009.11.003
Prats, X., Puig, V., Quevedo, J., Nejjari, F., 2010b. Multi-objective optimisation for aircraft departure trajectories minimising noise annoyance. Transp. Res. Part C Emerg. Technol. 18, 975–989. doi:10.1016/j.trc.2010.03.001
Southgate, D., 2011. The Evolution of Aircraft Noise Descriptors in Australia over the Past Decade, in: Proceedings of Acoustics. 2-4 November 2011, Gold Coast, Australia.
Torres, R., Chaptal, J., Bès, C., Hiriart-Urruty, J.-B., 2011. Optimal , Environmentally Friendly Departure Procedures for Civil Aircraft. J. Aircr. 48, 11–23. doi:10.2514/1.C031012

Visser, H.G., Wijnen, R.A.A., 2003. Optimisation of noise abatement arrival trajectories. Aeronaut. J. 107, 607–615. doi:10.1017/S0001924000013828
Visser, H.G., Wijnen, R.A.A., 2001. Optimization of Noise Abatement Departure Trajectories. J. Aircr. 38, 620–627. doi:10.2514/2.2838
Zachary, D.S., Gervais, J., Leopold, U., 2010. Multi-impact optimization to reduce aviation noise and emissions. Transp. Res. Part D Transp. Environ. 15, 82–93. doi:10.1016/j.trd.2009.09.005
Zhang, M., Filippone, A., Bojdo, N., 2016. Multi-objective departure trajectory optimisation of commercial aircraft on environmental impacts. Greener Aviation Conference, At Brussels, Belgium. doi:10.13140/RG.2.2.23283.32805
Zhang, Q., Li, H., 2007. MOEA/D: A Multiobjective Evolutionary Algorithm Based on Decomposition. IEEE Trans. Evol. Comput. 11, 712–731. doi:10.1109/TEVC.2007.892759